Spectrum of Engineering Sciences
ISSN (e) 3007-3138 (p) 3007-312X Volume 2, Issue 5, 2024

ANALYSIS OF THE COMPLEX PERMITTIVITY AND PERMEABILITY OF A MARTIAN SOIL FOR RADAR CROSS SECTION (RCS) INVESTIGATION OF PEC RECTANGULAR PLATE BETWEEN FREQUENCY : 10 MHz-1GHz.

M.Akbar[*1], Saeed Ahmed[2]

[*1]*Department of Physics, Air University, Islamabad, Pakistan,*
[2]*Department of Mathematics, Quaid-i-Azam University, Islamabad, Pakistan,*

[*1]akbar5508126@yahoo.com,[2]saeedqau@gmail.com

DOI:https://doi.org/10.5281/zenodo.17397038

Keywords
Radar Cross Section, Rectangular Plate, Lossy Medium, Complex permitittivity and permeability, Scattering Analysis.

Article History
Received on 20 November 2024
Accepted on 20 December 2024
Published on 27 December 2024

Corresponding Author: *
M.Akbar

Abstract
In this article, we investigate the RCS of a rectangular plate embedded in Martian soil. The motivation is to provide an analysis of the electrical properties, complex permittivity and permeability of a soil within the frequency range $(10 - 1000)MHz$ *that can be expected on the surface of Mars. These values will provide useful information concerning the performance of a ground-penetrating radar (GPR) on Mars. The results are presented over the frequency range of interest and numerical results are compared with the free space.*

INTRODUCTION

The problem discussed here, is the consequence of the results investigated in [1, 2] worked out for lossy medium. Probing of Subsurface Cavities is a great deal of interest in the possible application of electromagnetics (EM) commonly known as ground-probing radar. The radar cross section, $\sigma_{\mu\epsilon}$, is computed for an object in a lossy full halfspace. However, when the radar cross section is calculated from a scattered field by a PEC object in lossy medium, the losses must be carefully investigated from the definition of the cross section. When reflected signals are received, the range to a target can be calculated by determining the interval of the radar signalâ€™s travel; the half time of total interval gives the distance of the target while the radar signal propagates from the transmitter and returns to the receiver after reflection from the target. It can be used in civilian applications (Airport surveillance, Marine navigation, Weather Radar, Altimetry, Aircraft Landing, Security alarms, Speed measurement and Geographic mapping), Military applications (Air and marine navigation, Detection and tracking of aircraft, missiles, and super crafts, Fire control for missiles and artillery, and Reconnaissance), and Scientific application (Astronomy, Mapping and imaging, Precision distance measurement and Remote sensing of the environment) etc. A target is located by the radar only when the radarâ€™s receiver gets adequate energy back from the target [3]. The information of

RCS characteristics of some simple targets is very essential in RCS measurement and analysis of complex targets. Complex targets such as missiles, ships, aircrafts etc., can be described as collections of relatively simple shapes like spheres, flat plates, cylinders, cones and corner reflectors. The RCS depends upon the material, size, relative size to wavelength, shape of target, and the incident angle at which beam hits a particular portion of the target. This problem has been solved [4] by the Physical Optics (PO) method that calculates the surface current induced on an arbitrary body by the incident radiation. On the portions of the object that are directly illuminated by the incident field, the induced current is simply proportional to the incident magnetic field intensity. On the shadowed portion of the target, the current is set to zero. The current is then used in the radiation integrals to compute the scattered field far from the target. This method is a high frequency approximation that provides the best results for electrically large targets as well as in the specular direction [6, 7, 8, 9]. Physical optics is derived from Maxwellâ€™s equations [5]. Radar Cross-Section has been written as the ratio of radiated power density intercepted by a target to the power per unit solid angle backscattered to the receiving antenna by the target. Its performance depends on shape, size, material composition, frequency, aspect angle, surface area and other factors that vary widely between different types of target. The ability of the radar to detect and analyze the shape, range, effective capture area and size of an object is the chief attributes of the Radar Cross Section (RCS) [4].

The moisture content of the earth material is the single most important factor affecting EM absorption loss. An increase in moisture content of the soil or other earth material greatly increases both the electrical conductivity and the dielectric constant of the earth. The dielectric constant normally used for ground-penetrating radar frequencies is generally in the range of 3 to 30. Radar imaging and detection of targets buried in soil has wide applications in the different areas. First, it is necessary to understand how the soil responds to EM wave and how targets buried within the soil scatter it. We examine the response of the soil to a short pulse, and illustrate the roll of the complex dielectric permittivity of the soil in determining radar range resolution. This leads to a concept of an optimum frequency and bandwidth for imaging in a particular soil. The radar cross section RCS of several canonical objects in lossy media is investigated and and GPR method is used by several authors [10, 11, 12, 13, 14, 15, 16, 17, 18, 19, 20, 21, 22, 23, 24, 25, ?, 26, 27, 28, 29, 30, 31, 32, 33, 34, 35, 36, 37, 38, 39, 40, ?, 41, 42, 43, 44, 45, 46, 47, 48], who have worked out electromagnetic problems concerned with lossy medium by using approximate values of conductivity and dielectric constants of various materials. In this problem, we are going to investigate RCS of a rectangular plate by the characterisitcs of Martian Soil. This has been solved by the Physical Optics (PO) method as in the published work [1, 2]. Here, we will follow two soil models, one for the permittivity of the Martian Soil and the other one is the permeability of the Martian Soil within the frequency range $(10 - 1000)$ MHz.

2. Materials and methods

First, we give an introduction to scattering width (RCS) of PEC rectangular plate in lossy medium. Secondly, we calculate the scattering width of PEC rectangular plate embedded in Martian Soil. The radar cross section,$\sigma_{\mu\epsilon}$, is defined as

$$\sigma_{\mu\varepsilon} = \lim_{R\to\infty} 4\pi R^2 \frac{\left|e^{|Im(\vec{K}.(\vec{R}-\vec{a}))|}\vec{E}_s\right|^2}{\left|\vec{E}_i e^{|Im(\vec{K}.\vec{a})|}\right|^2} \quad (1)$$

The RCS of PEC rectangular plate for the following two models of soil is investigated. These models for radar cross section will find considerable utility in estimating target brightness. The scattered field used in the definition of the radar cross section,$\sigma_{\mu\epsilon}$, will be based on uniform plane-wave scattering from a PEC

plate. Now Consider the formulation of the problem in which scattering from a three dimensional PEC rectangular flate plate embedded in lossy medium that is illuminited by a uniform plane wave. The problem has been solved by following method given in Balani [3]. The incident plane wave is assumed to have TE^x polarization and lies on the $\hat{y}-\hat{z}$ plane. The incident electric and magnetic field can be represented as

$$E^i = \eta H_0(\hat{y}\cos\theta_i + \hat{z}\sin\theta_i)e^{-i\gamma(y\sin\theta_i - z\cos\theta_i)} \quad (2)$$

and

$$H^i = \hat{x}H_0 e^{-i\gamma(y\sin\theta_i - z\cos\theta_i)} \quad (3)$$

where

$$\gamma = \beta - i\alpha$$

in which real part β is interpreted as the phase constant, and the imaginary part α is the attenuation constant. where

$$\alpha = \omega\sqrt{\epsilon_0\mu_0}\sqrt{\frac{\epsilon_r}{2}}\left[\sqrt{1+\left(\frac{18\sigma}{\omega\epsilon_r\epsilon_0}\right)^2}-1\right]^{1/2}$$

$$\beta = \omega\sqrt{\epsilon_0\mu_0}\sqrt{\frac{\epsilon_r}{2}}\left[\sqrt{1+\left(\frac{18\sigma}{\omega\epsilon_r\epsilon_0}\right)^2}+1\right]^{1/2}$$

here σ is the conductivity of soil, ϵ_0 is the permittivity of free space and ϵ_r is the relative permittivity of soil.

In this paper we use a simple Debye-Pellat relaxation equation as a model for the frequency dependency of the permittivity and permeability of the soil simulant. The models are written in terms of the complex permittivity and permeability as

$$\epsilon' - j\epsilon'' = \epsilon_\infty + \frac{\epsilon_s - \epsilon_\infty}{1+j\omega\tau_\epsilon} \quad (4)$$

$$\mu' - j\mu'' = \mu_\infty + \frac{\mu_s - \mu_\infty}{1+j\omega\tau_\mu} \quad (5)$$

where $\epsilon_r = \epsilon' - j\epsilon''$ and $\mu_r = \mu' - j\mu''$

Table 1

Soil parameters and least error values

Soil Parameters	Description	values
ϵ_∞	Permittivity at Infinity	3.12
ϵ_s	Static Permittivity (d.c.)	3.57
τ_ϵ	Permittivity Relaxation Time	0.041 ns
μ_∞	Permeability at Infinity	1.01
μ_s	Static Permeability	1.2
τ_μ	Permeability Relaxation Time	0.2 ns

The total scattered fields [1, 2, 7] are given as

$$E^s = -i\omega A - i\frac{1}{\omega\mu\epsilon}\nabla(\nabla.A) - \frac{1}{\epsilon}\nabla \times F \quad (6)$$

$$H^s = \frac{1}{\mu}\nabla \times A - -i\omega F - i\frac{1}{\omega\mu\epsilon}\nabla(\nabla.F) \quad (7)$$

where A and F are the magnetic and electric vector potentials, respectively and can be determined by using the following formulae

$$A = \frac{\mu}{4\pi}\int\int\int_v J(x',y',z')\frac{e^{ikr}}{r}dv' \quad (8)$$

and

$$F = \frac{\epsilon}{4\pi}\int\int\int_v M(x',y',z')\frac{e^{ikr}}{r}dv' \quad (9)$$

in which J and M are the electric and magnetic current densities respectivel. Here, the radial component of electric and magnetic fields become negligible.

$$E_r = 0 \quad (10)$$

$$E_\theta = -i\omega\left(A_\theta + \eta F_\phi\right) \quad (11)$$

$$E_\phi = -i\omega\left(A_\phi - \eta F_\theta\right) \quad (12)$$

$$H_r = 0 \quad (13)$$

$$H_\theta = \frac{i\omega}{\eta}\left(A_\phi - \eta F_\theta\right) \quad (14)$$

$$H_\phi = -\frac{i\omega}{\eta}\left(A_\theta + \eta F_\phi\right) \quad (15)$$

in which the vector potential components have also simplified as

$$A_\theta = \frac{\mu e^{-i\gamma r}}{4\pi r}N_\theta \quad (16)$$

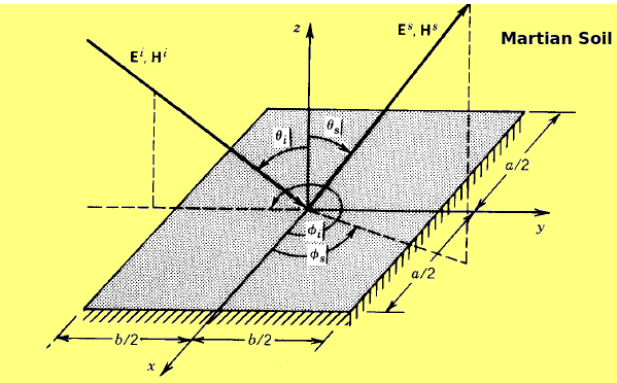

Figure 1: Uniform plane wave incident on perfectly conducting, rectangular flat plate embedded in Matian Soil.

$$A_\phi = \frac{\mu e^{-i\gamma r}}{4\pi r}N_\phi \quad (17)$$

$$F_\theta = \frac{\epsilon e^{-i\gamma r}}{4\pi r}L_\theta \quad (18)$$

$$F_\phi = \frac{\epsilon e^{-i\gamma r}}{4\pi r}L_\phi \quad (19)$$

where N_θ, N_ϕ, L_θ, and L_ϕ can be determined from [1, 7]

Here, the magnetic current densityy M is zero, such that $L_\theta = L_\phi = 0$.

Using the physical optic approximation, the current density J induced on the surface of the plate by the incident plane wave denoted by

$$J_s = 2\hat{z} \times H^i|_{z=0,y=y'} = 2\hat{y}H_0 e^{-i\gamma y' \sin\theta_i} \quad (20)$$

By simplifying the mathematical expresssions, we find

$$E_\theta^s \cong j\eta \frac{\gamma H_0}{2\pi r}(aY\cos\theta_s)e^{-j\gamma r}$$

where

$$Y = \frac{j}{\beta' - j\alpha'}\left[e^{-\frac{b}{2}(\alpha' + j\beta')} - e^{\frac{b}{2}(\alpha' + j\beta')}\right]$$

$$\alpha' = \alpha(\sin\theta_s \sin\phi_s - \sin\theta_i)$$

and

$$\beta' = \beta(\sin\theta_s \sin\phi_s - \sin\theta_i)$$

. The plane of incident electromagnetic field for this problem defined as $\phi_i = \frac{3\pi}{2}$, $0 \le \theta_i \le \frac{\pi}{2}$. To get the monostatic backscattered field from the plate means that $\phi_s = \phi_i = \frac{3\pi}{2}$ and $\theta_s = \theta_i$, hence $E_\phi^s \cong 0$, thus only the total scattered field equals to E_θ^s and the scattering width (RCS) can be written as

$$\sigma_{\mu\epsilon} = \begin{cases} \frac{a^2}{\pi}\left|\gamma Y e^{-2d|Im(\gamma)|}\right|^2 \cos^2\theta_s & \text{if} \theta_s \neq 0 \\ \frac{a^2 b^2}{\pi}|\gamma|^2 & \text{if} \theta_s = 0 \end{cases}$$

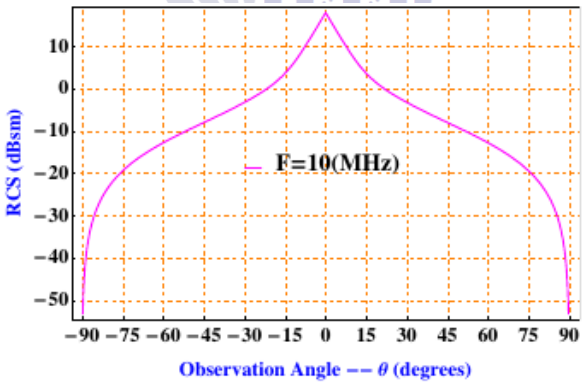

Figure 2: This shows the scattering width of plate for frequency $f = 10MHz$

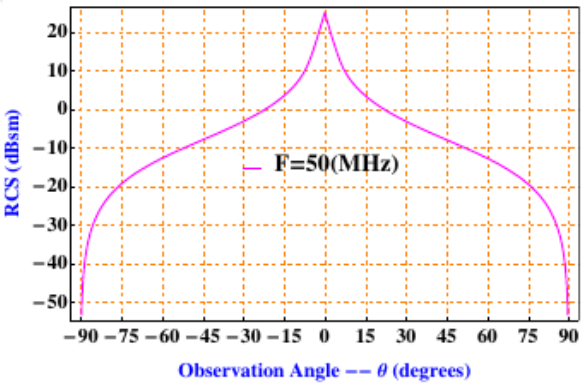

Figure 3: This shows the scattering width of plate for frequency $f = 50MHz$.

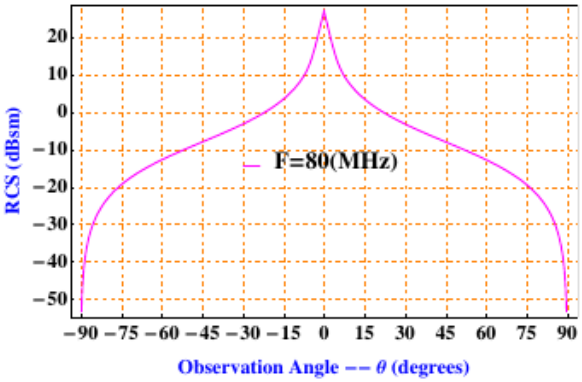

Figure 4: This shows the scattering width of plate shows the variation in RCS for $f = 80MHz$

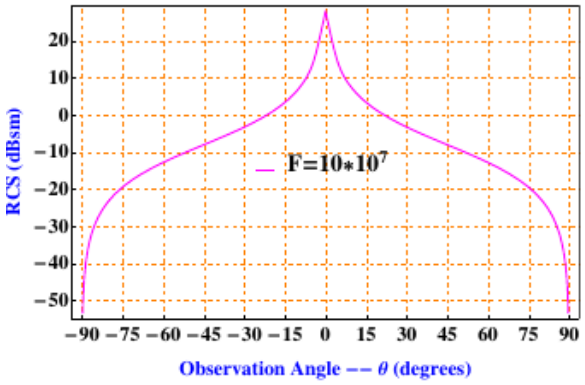

Figure 5: This shows the scattering width of plate shows the variation in RCS for $f = 100MHz$

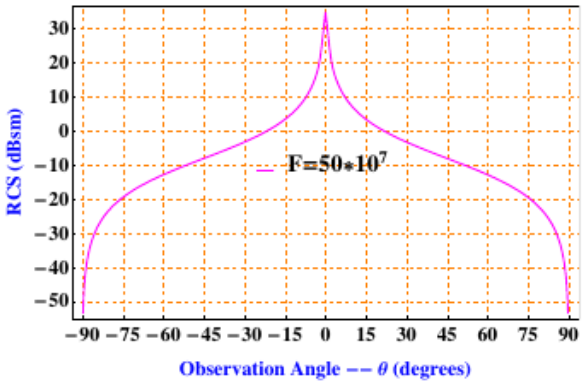

Figure 6: This shows the scattering width of plate shows the variation in RCS for $f = 500MHz$

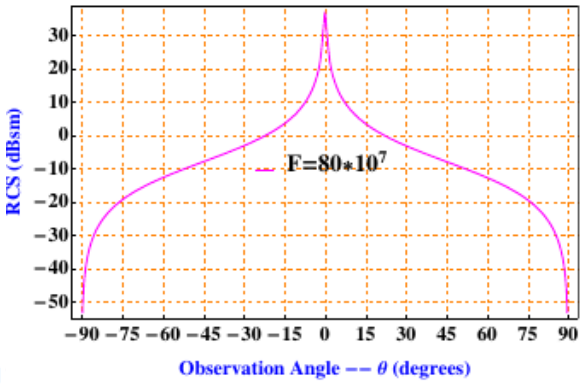

Figure 7: This shows the scattering width of plate shows the variation in RCS for $f = 800MHz$

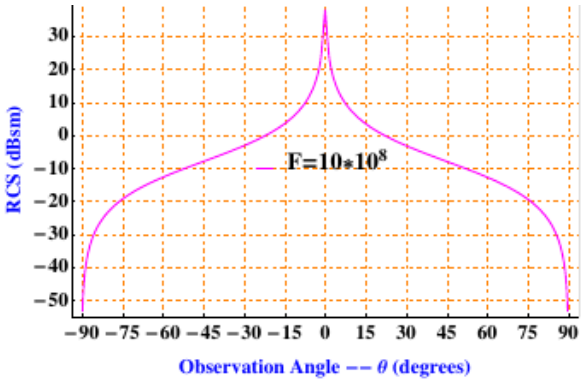

Figure 7: This shows the scattering width of plate shows the variation in RCS for $f = 1000MHz$

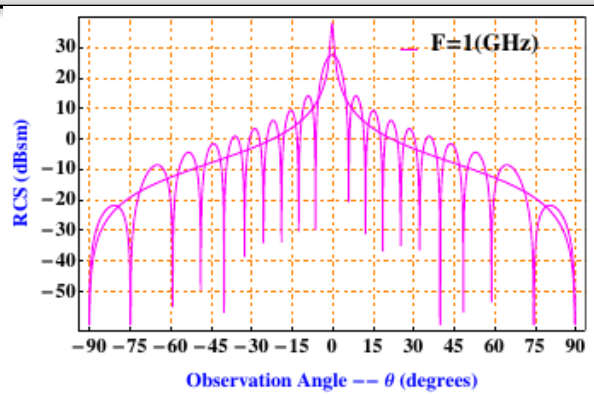

Figure 9: This shows the scattering width of plate shows the variation in RCS for $f = 10000MHz$

3. Data Analysis and Results

The radar cross section is computed for $5\lambda_0 \times 5\lambda_0$ rectangular flat plate embedded in four different types of lossy soil models as defined in Table 1, where λ_0 is free space wavelength. The maximum of the scattered field from the flat plate embedded in the lossy media becomes larger as the frequecy increases. A complete description of the model for the soil electric and magnetic constants are contained in [39], while the dielectric soil models can be briefly described here as

$$\epsilon' - j\epsilon'' = \epsilon_\infty + \frac{\epsilon_s - \epsilon_\infty}{1 + j\omega\tau_\epsilon} \quad (21)$$

$$\mu' - j\mu'' = \mu_\infty + \frac{\mu_s - \mu_\infty}{1 + j\omega\tau_\mu} \quad (22)$$

where $\epsilon_r = \epsilon' - j\epsilon''$ and $\mu_r = \mu' - j\mu''$, such that

$$\epsilon = \epsilon_r \epsilon_0 \quad (23)$$

and

$$\mu = \mu_r \mu_0 \quad (24)$$

. The characteristic impedance can be expressed as

$$Z = \sqrt{\frac{\mu_r}{\epsilon_r}} Z_0$$

, where $Z_0 = 50$ ohm and the conductivity σ is assumed to be $\frac{1}{Z}$, where ϵ_r and μ_r are the complex permittivity and permeability of the soil simulant [39], respectively. Using the Mathematica, we have evaluated scattering width by taking the numeric values of propagation constant and attenuation constant as well as ϵ_r and μ_r from the given table [39]. The Scattering width of PEC rectangular plate embedded in the Martian Soil versus observation angle have been visualized for different frequencies corresponding to relevant σ, ϵ_r and μ_r. Figure (a) shows a variation in RCS for $f = 10MHz$, (b) shows a variation in RCS for $f = 50MHz$, (c) shows a scattering width of plate for frequency $f = 80MHz$, (d) shows a variation in RCS for $f = 100MHz$, (e) shows a variation in RCS for $f = 500MHz$, (f) shows a variation in RCS for $f = 700MHz$, (g) shows a variation in RCS for $f = 800MHz$, (h) shows a variation in RCS for $f = 900MHz$, and (i) shows a variation in RCS for $f = 1GHz$, and (j) shows a variation in RCS for $f = 1GHz$ and comparison with free space. Behavior of the RCS of the rectangular plate embedded in Martian Soil predicts that as we increase frequency from $(10 - 1000)$ MHz, the amplitude of the RCS increases versus the observation angle. Finally we have compared the results of the

RCS of the rectangular plate embedded in the lossy medium with the rectangular plate place in free space. The results show the validity of the given plots in the article.

3. CONCLUSION

The ability of the Radar system is to detect and analyze the shape, range, effective capture area and size of an object depends on the Radar Cross Section (RCS), thus, it became pertinent at the design phase of the Radar system to employ computer simulation software through which the analysis of the complex permittivity and permeability of a martian soil for RCS of PEC Rectangular Plate from 10 MHz to 1 GHz, predicts that the amplitude of the RCS increases as frequency increases.

5 Acknowledegment

The authors are thankful to the anonymous referees for their valuable suggestions to improve the quality of the paper.

REFERENCES

[1] Saeed Ahmed, Muhammad Khalid khan and Atta ur Rehman, Scattering by a perfect electromagnetic conductor plate embedded in lossy medium, *International Journal of Electronics*, Vol. 103, Issue: 07, pages 1228 - 1235, 2015.

[2] C. A. Balanis, Advanced Engineering Electromagnetics, John Wiley & Sons, New York,1989.

[3] Edde, B. (1993). Radar-Principles, Technology, Applications, Prentice-Hall, Englewood Cliffs, NJ.pp.78-89.

[4] Knott E.F., Shaeffer J.F., Tuley M.T. (2004), Radar Cross Section, Second Edition. SciTech Publishing, Raleigh, NC, USA, Pp. 1-21 and 115-223.

[5] Jansen C., Krumbholz N., Geise R., Enders A., Koch M. (2009), Scaled radar cross section measurements with terahertz-spectroscopy up to 800 GHz, European Conference on Antennas and Propagation, Berlin, Germany. Pp. 3645-3648.

[6] Skolnik M. I. (2008), Radar Handbook, Third Edition. McGraw-Hill Companies, New York, USA, Pp. 12-34.

[7] D J. Daniels, Ground Penetrating Radar, IET, 2004.

[8] George T. Ruck, Radar Cross Section Handbook, Plenum Press, 1970.

[9] Fang C. H., Zhao X. N., and Liu Q. (2008), "An Improved Physical Optics Method for the Computation of Radar Cross Section of Electrically Large Objects", Asia-Pacific Symposium on Electromagnetic Compatibility & 19th International Zurich Symposium on Electromagnetic Compatibility, Singapore. Pp.722-725.

[10] B. C. Brock and K. W. Sorensen, "Electromagnetic Scattering from Buried Objects,"Sandia National Laboratories, SAND94-2361, Sept., 1994.

[11] B. C. Brock, W. E. Patitz, Optimum Frequency for Subsurface-Imaging Synthetic Aperture Radar, SAND93-0815, May 1993.

[12] A. W. Doerry, A Model for Forming Airborne Synthetic Aperture Radar Images of Underground Targets, SAND94-0139, January 1994.

[13] Kuloglu, M., Chi-Chih Chen, "Ground penetrating radar for tunnel detection", Geoscience and Remote Sensing Symposium (IGARSS), IEEE International, pages:4314-4317, 2010.

[14] J. D. Jackson, Classical Electrodynamics, John Wiley & Sons, Inc., New York, 1962.

[15] M. Abramowitz, I. Stegun, Handbook of Mathematical Functions with Formulas, Graphs, and Mathematical Tables, Dover Publications, Inc., New York, 1972 (originally published by the National Bureau of Standards, 1964).

[16] J. Mathews, R. L. Walker, Mathematical Methods of Physics, second edition, The BenjamidCummings Publishing Company, Menlo Park, 1970.

[17] A. R. Von Hippel, ed., Dielectric Materials and Applications, The Technology Press of M.I.T., and John Wiley & Sons, Inc., New York, 1954.

[18] B. O. Peirce, A Short Table of Integrals, Fourth Edition, Ginn and Company, Boston, 1956.

[19] R. F. Harrington, Time-Harmonic Electromagnetic Fields, McGraw-Hill Book Company, New York, 1961.

[20] J. E. Hipp, "Soil Electromagnetic Parameters as Functions of Frequency, Soil Density, and Soil Moisture", Proceedings of the IEEE, vol. 62, no. 1, January 1974, pp. 98-103.

[21] S. J. Radzevicius and J. J. Daniels, â€œGround penetrating radar polarization and scattering from cylinders, Journal of Applied Geophysics, vol. 45, pp. 111-125, 2000.

[22] B.A. Kramer, C-C. Chen, M. Lee, and J. L. Volakis, Fundamental limits and design guidelines for miniaturizing ultrawideband antennas, IEEE Antennas and Propagation Magazine, vol. 51, pp. 57-69, 2009.

[23] J.O. Curtis, A durable laboratory apparatus for the measurement of soil dielectric properties,â€ Instrumentation and Measurement, IEEE Transactions on, vol. 50, no. 5, pp. 1364-1369, oct 2001.

[24] Saeed Ahmed, The study of the radar cross section of perfect electromagnetic conductor strip, *Optik.*, Vol. 126, 23, 4191-4194, December 2015.

[25] Saeed Ahmed, Muhammad Khalid khan and Atta ur Rehman, Scattering by a perfect electromagnetic conductor plate embedded in lossy medium, *International Journal of Electronics*, Vol. 103, Issue: 07, pages 1228-1235, 2015.

[26] Plessix, R. E., P. Milchik, H. Rynja, A. Stopin, and K. Matson, 2013, Multiparameter full-waveform inversion: Marine and land examples: TheLeading Edge, 32, 1030-1038.

[27] Tsoflias, G. P., and M. W. Becker, 2008, Ground-penetrating radar response to fracture-fluid salinity: Why lower frequencies are favorable for resolving salinity changes: Geophysics, 73, no. 5, J25-J30, doi: 10.1190/1.2957893.

[28] Klotzsche, A., J. van der Kruk, G. A. Meles, J. Doetsch, H. Maurer, and N. Linde, 2010, Full-waveform inversion of cross-hole ground-penetrating radar data to characterize a gravel aquifer close to the Thur River, Switzer- land: Near Surface Geophysics, 8, 635-649, doi: 10.3997/1873-0604.2010054.

[29] Kalogeropoulos, A., J. van der Kruk, J. Hugenschmidt, J. Bikowski, and E. Bruhwiler, 2013, Full-waveform GPR inversion to assess chloride gradients in concrete: NDT & E International, 57, 74-84, doi: 10.1016/j.ndteint.2013.03.003.

[30] Guha, S., S. E. Kruse, E. E. Wright, and U. E. Kruse, 2005, Spectral analysis of ground penetrating radar response to thin sedimentary layers: Geophysical Research Letters, 32, L23-304.

[31] Carcione, J. M., G. Seriani, and D. Gei, 2003, Acoustic and electromagnetic properties of soil saturated with salt water and NAPL: Journal of Applied Geophysics, 52, 177-191, doi: 10.1016/S0926-9851(03)00012-0.

[32] Busch, S., J. van der Kruk, J. Bikowski, and H. Vereecken, 2012, Quantitative conductivity and permittivity estimation using full-waveform inversion of on-ground GPR data: Geophysics, 77, no. 6, H79-H91.

[33] Bradford, J. H., D. F. Dickins, and P. J. Brandvik, 2010, Assessing the potential to detect oil spills in and under snow using airborne ground-penetrating radar: Geophysics, 75, no. 2, G1-G12, doi: 10.1190/1.3312184.

[34] Bradford, J. H., W. P. Clement, and W. Barrash, 2009, Estimating porosity with ground-penetrating radar reflection tomography: A controlled 3-D experiment at the Boise Hydrogeophysical Research Site: Water Resources Research, 45, W00D26, doi: 10.1029/2008WR006960.

[35] Bradford, J. H., 2007, Frequency-dependent attenuation analysis of ground penetrating radar data: Geophysics, 72, no. 3, J7-J16, doi: 10.1190/1.2710183.

[36] Bradford, J. H., and J. C. Deeds, 2006, Ground-penetrating radar theory and application of thin-bed offset-dependent reflectivity: Geophysics, 71, no. 3, K47-K57, doi: 10.1190/1.2194524.

[37] F. Frezza, L. Pajewski, C. Ponti, G. Schettini and N. Tedeschi, Cylindrical-Wave Approach for electromagnetic scattering by subsurface metallic targets in a lossy mediumâ€, Journal of Applied Geophysics 97 (2013) 55-59.

[38] Armin W. Doerry, A Model for Forming Airborne Synthetic Aperture Radar Images of Underground Targets, Synthetic Aperture Radar Department, 2345, Sandia National

Laboratories Albuquerque, NM 87185-0529, Technical Report, January 1994.
[39] Carl Leuschen, Analysis of the Complex Permittivity ancl Permeability of a Martian Soil Simulant, Proc. 1999 Geoscience and Remote Sensing Symposium, 4:2264-2266.
[40] P. Rajyalakshmi and G.S.N. Raju, Characteristics of Radar Cross Section with Different Objects , International Journal of Electronics and Communication Engineering, ISSN 0974-2166 Volume 4, Number 2 (2011), pp. 205-216.
[41] Lingfei CHENG, Xinhang BAO and Chao LU, Influence of the Shape Factor on Electromagnetic Waves Propagation in Tunnels, Journal of Computational Information Systems 9: 24 (2013) 9885-9891.
[42] Timothy W. Miller, RADAR DETECTION OF BURIED LANDMINES IN FIELD SOILS, MS Thesis in Hydrology, New Mexico Institute of Mining and Technology Socorro, New Mexico, August 2002.
[43] K. Rama Rao, K.-H. Lee, C-C. Chen and R. Lee, â€œApplication of Full-Polarimetric Groung Penetrating Radar for Buried UXO Classification,â€ Technical Report, 738520-1, The Ohio State University, ElectroScience Laboratory, Feb. 2001. [44] Robert F. Ballard Jr., ELECTROMAGNETIC (RADAR) TECHNIQUES APPLIED TO CAVITY DETECTION, Technical Report No. 5, Geotechnical Laboratory, P.O. BOX 631, Vicksburg, Miss. 39180, July 1983.
[45] S. J. Radzevicius and J. J. Daniels, â€œGround penetrating radar polarization and scattering from cylinders, Journal of Applied Geophysics, vol. 45, pp. 111-125, 2000.
[46] ZHENHUA MA, ADVANCED FEATURE BASED TECHNIQUES FOR LANDMINE DETECTION USING GROUND PENETRATING RADAR, MS Thesis, University of Missouri-Columbia, 2007.
[47] Remke L, Van Dam, causes of ground-penetrating radar reflections in sediment, Ph. D Thesis, Faculty of Earth Scinces, Virje Universiteit, 1081 Amsterdam, Netherland, 17 December 2001.
[48] Haoping Huang and I. J. Won, Electromagnetic detection of buried metallic objects using quad-quad conductivity, GEOPHYSICS, VOL. 69, NO. 6 (NOVEMBER-DECEMBER 2004),Pp. 1387-1393.